J. Plasma Fusion Res. SERIES, Vol. 5 (2002) 337–341

Recent Progress of the High Power ECRF System on JT-60U

SEKI Masami, MORIYAMA Shinichi, KAJIWARA Ken, IKEDA Yoshitaka,
SAKAMOTO Keishi, IMAI Tsuyoshi and FUJII Tsuneyuki
Naka Fusion Research Establishment, Japan Atomic Energy Research Institute,
Naka, Ibaraki 311-0193, Japan

(Received: 11 December 2001 / Accepted: 12 November 2002)

Abstract

The Electron Cyclotron Range of Frequency (ECRF) system having four 1 MW – gyrotrons has been successfully operated on JT-60U to locally heat a plasma and drive a plasma current. After modification by suppressing a parasitic oscillation, the gyrotron can generate ~1.1 MW power for 3.2 s. High RF powers generated by four gyrotrons are transmitted to two independent antennas consisting of steerable mirrors via four long transmission lines with moderate transmission efficiency of 70–80 %. In 2001, injected power reaches up to ~2.8 MW for 2.8 s after optimizing operational parameters. In such high power injection, a substantial increment in the central electron temperature from 5 keV up to ~13 keV is observed in the Reversed-Shear (R-S) plasma with the Internal Transport Barrier (ITB).

Keywords:

ECRF, JT-60U, plasma heating, current drive, gyrotron, high power injection

1. Introduction

Electron cyclotron (EC) waves play important and useful roles of heating (ECH), current drive (ECCD) and start-up assist not only in tokamaks but also in other fusion devices. Especially a local current drive by EC waves can stabilize MHD instabilities. Moreover, EC waves have an advantage of propagating in vacuum, so the antenna can be set far away from plasma.

Development of gyrotrons at a frequency of over 100 GHz has made good progress in the past several years. The Collector Potential Depression (CPD) technology for the gyrotron has improved efficiency [1]. A diamond window enabled steady state operation of the gyrotron due to its low RF loss and high thermal conductivity [2]. One ECRF unit, which was composed of a 110 GHz CPD gyrotron, power supply system, a transmission line and an antenna, was constructed in 1999 [3]. A 1 MW oscillation of the CPD gyrotron was obtained on the main DC power supply with stability of ±1 % by keeping high stability of ±0.5 % in the acceleration voltage. The diamond window of the gyrotron also enabled the gaussian output mode, which was effective for conversion to low loss HE_{11} mode in the transmission line [4]. In 2000, three gyrotrons were operated to ECH / ECCD at the injection power level of 1.5~1.6 MW [5]. In 2001, the ECRF system in JT-60U has been completed to be a 4 MW-110 GHz system for a wide variety of ECH/ECCD investigations such as on/off-axis and co/counter injections.

This paper gives an overview of the high power ECRF system and recent progress through experience of operation in Section **2** and **3**, respectively. Section **4** and 5 show the typical result of high power heating and the summary.

Corresponding author's e-mail: seki@naka.jaeri.go.jp

2. Overview of the ECRF System on JT-60U

The ECRF system consists of four independent units as shown in Fig. 1. Each unit can generate a high output power around 1 MW by the high power gyrotron at a working frequency of 110 GHz. The gyrotron in each unit is featured by the Collector Potential Depression (CPD) technology. The CPD technique is to recover the kinetic energy of the spent electron beam by depressing the voltage between the body and collector section of the gyrotron. The CPD technology also allows a stable operation of the gyrotron by the combination of the main DC voltage supply system and the stable Acceleration Power Supply (APS). The APS can give an acceleration voltage between the cathode and the body sections up to 100 kV, 300 mA within high stability of ±0.5 %. Since the APS is applied in floating to the cathode voltage fed by the main DC power supply (–60 kV), the acceleration voltage (~+85 kV) between the cathode and body section can be constant even if the main DC voltage is fluctuated. The gyrotron oscillation mode of $TE_{22,6}$ is converted to a gaussian mode. The output window employs a single CVD diamond disk with an outer diameter of 96 mm, allowing it to continuously transmit the gaussian beam at the power level of 1 MW.

There are four transmission lines, each of which has basically the same combination of RF components as shown in Fig. 1. The total length from the gyrotron to the antenna is about 60 m. The transmission line is evacuated to avoid RF breakdowns in it. The gaussian mode from the gyrotron output window is converted to the low-loss HE_{11} mode in the transmission line using two phase-corrected mirrors in a Matching Optical Unit (MOU). The transmission line is mainly composed of a corrugated waveguide with a diameter of 31.75 mm. There are directional couplers to detect RF power at the outlet of the gyrotron and at the inlet of the antenna. A pair of polarizers is used to change the polarization of the transmitted wave. A 1 MW × 3 s dummy load is installed for conditioning the gyrotron. The diamond window is installed near the antenna for the vacuum boundary.

One of the major aims of the ECRF system is to locally drive a plasma current and to control its position within about ~0.1 m for suppression of MHD instabilities. Therefore an injection angle of the RF beam should be controlled. There are two antennas on the system, so called antenna-A and antenna-B. Antenna-A is connected with three units to control the poloidal injection angle at the fixed toroidal injection angle of ~20°. Antenna-B is connected with unit 4 to control the injection angle in toroidal/poloidal directions with two steerable mirrors [6].

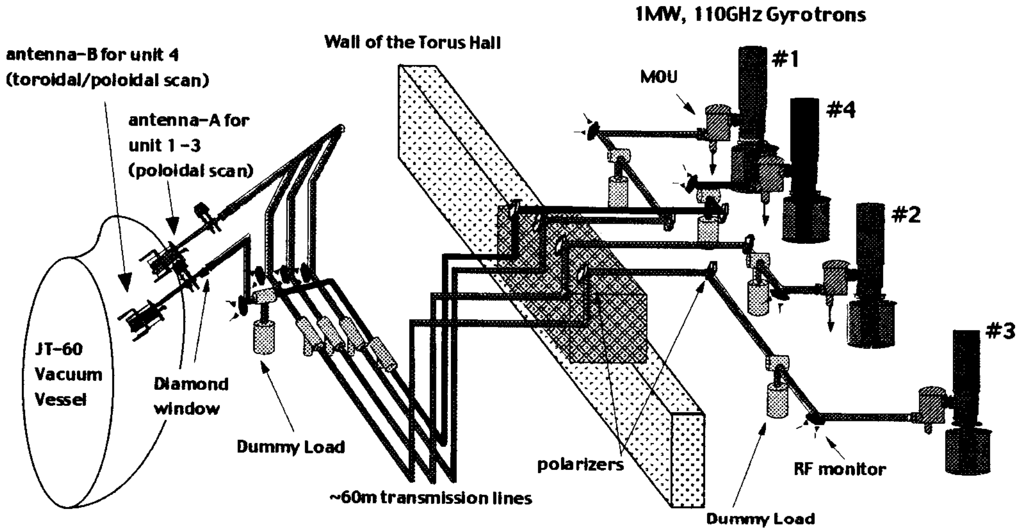

Fig. 1 Layout of the ECRF system on JT-60U.

3. Progresses of the ECRF System

3.1 Optimization of Start-up Speed of APS

The CPD gyrotron worked on the combination of the main DC voltage power supply system and the APS, however, a large fluctuation was observed in the CPD voltage ($V_{CPD} = V_{acc} + V_{cathode}$) when the start-up speed of the APS was set at ~10 ms as shown in Fig. 2. Breakdown in the gyrotron often occurred at the moment when the CDP voltage was beyond the critical level (~30 kV). When V_{CPD} reached the level, spent electrons seemed to flow back to the body much more and as a result the over-current interlock acting in the APS. The over-current limited the APS voltage for high power operation. To suppress the over-shoot in V_{CPD}, the start-up speed of the APS was optimized from 10 to 50 ms. Thus the stable oscillation has been realized at the high APS voltage of 85–90 kV.

3.2 Increment of Transmission Efficiency

The RF loss of the long transmission line was measured by installing a calorimetric dummy load at the inlet of the antenna. In 2000, the transmission efficiencies including the mode conversion loss in MOU were measured and found to be ~75 %, ~70 % and ~60 % for unit 1, 2 and 3, respectively. A misalignment of 10 mm (displacement)/10 m (in length) was locally found in the transmission line of unit 3. Such misalignment seemed to degrade the transmission efficiency by undesired RF loss due to tilt effect. In 2001, re-alignments (less than ~2 mm/10 m) of the transmission lines have been performed for unit 2 and 3, then the re-alignments improve the transmission efficiencies to a level from ~70 % to ~75 % and from ~60 % to ~80 %, respectively. These moderate transmission efficiencies were close to the optimal of 81 %.

One of the main issues for long pulse operation is the over-heat of the transmission components such as miter bends, diamond windows and corrugated waveguides. The temperature was measured using thermocouples and was consistent with the prediction, which indicates the RF components is capable of transmitting a power of 0.8 MW (power density: ~1000 MW/m^2) for long pulse operation.

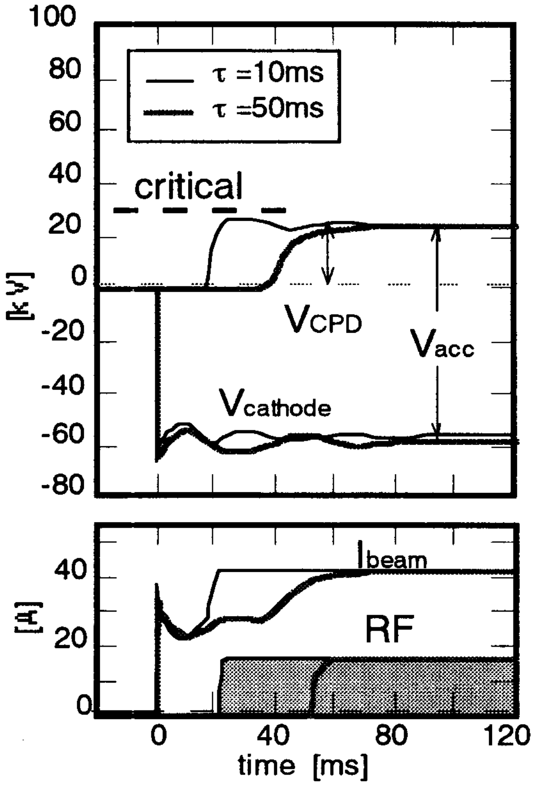

Fig. 2 Stabilization of the APS at start-up. Overshoot was observed in the V_{CPD} for the start-up time constant of 10ms compared with that of 50 ms.

3.3 Improvement of the Gyrotron

One major problem in the previous gyrotron operation was the increment of beam current during oscillation. Typical waveforms of the beam current are shown in Fig. 3. The oscillation was terminated by the

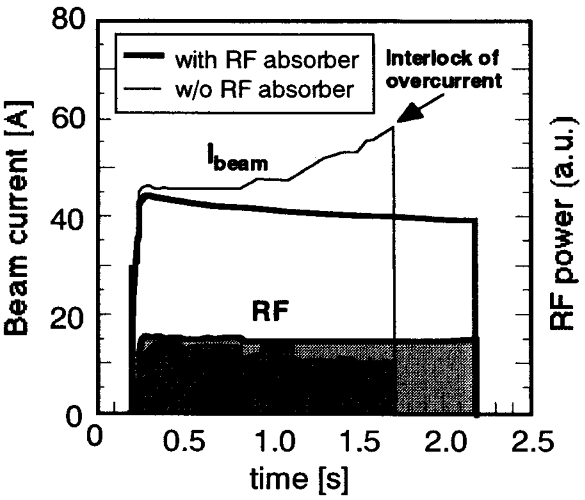

Fig. 3 Typical time evolution of beam current I_{beam} and RF power with / without RF absorber. The beam current I_{beam} increases in the case without RF absorber.

interlock of the beam over-current in this shot. It was found that the abrupt increment of the beam current was brought by the temperature rise of cathode surface due to a parasitic oscillation in beam tunnel. Moreover, the parasitic oscillation damaged a ceramic of the electron gun. After several shots of 3-second pulse, a vacuum leakage occurred in the gyrotron due to a crack in the ceramic.

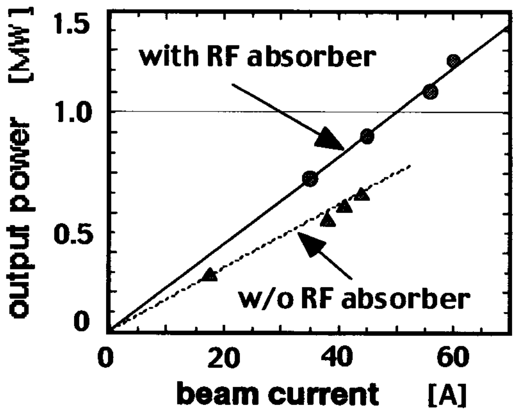

Fig. 4 Relation of the RF output power with the beam current. The RF output power increase with the beam current.

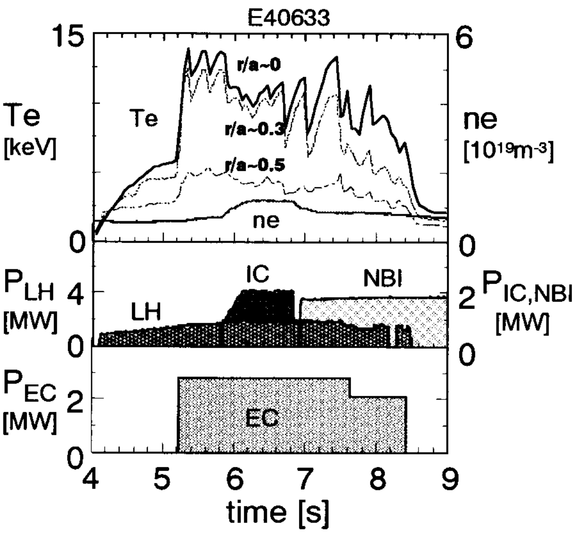

Fig. 5 Electron heating experiment by high ECRF power injection in R-S plasma. The LH power is injected for formation of the R-S plasma. IC power is injected to interact with high temperature electrons produced by EC heating.

The parasitic oscillation has been successfully suppressed by installing an SiC ceramic (RF absorber) on the inner wall of the beam tunnel [7]. The beam current does not increase and rather slightly decreases. Stable oscillation continues up to 3.2 s at output power of 1.1 MW even for such slightly decreasing beam current. The output power increases with the beam current at this stable phase as shown Fig. 4. The output power is expanded to ~1.3 MW (for 0.1 s) with the RF absorber while it was limited to 1 MW for 2 s without the RF absorber. The performance of improved gyrotrons has been extending through adequate conditioning.

4. Typical Result of High Power Heating

A typical result of heating experiments using the ECRF system is shown in Fig. 5. An RF power of ECRF is injected into a reversed-shear plasma with ITB initiated by the Lower Hybrid (LH) current drive during a plasma-current ramp-up. In this shot, an ECH power of ~2.8 MW is injected to obtain high temperature electrons, so that the central electron temperature within r/a ~0.3 measured by the polycrometer ECE increases from ~5 keV to ~13 keV by on-axis ECRF heating. The YAG Thomson measurement also shows the same efficient electron heating. In the same shot, Ion Cyclotron (IC) wave is launched to investigate the interaction between the fast waves of IC and high temperature electrons produced by EC heating, and a Neutral Beam (NBI) is injected to measure ion temperature for charge exchange recombination spectroscopy.

5. Summary

The high power ECRF system was constructed on JT-60U, having a capability of high output power up to 4 MW for several seconds using four CPD-gyrotrons at 110 GHz. By optimizing the start-up speed for the APS from 10 to 50 ms to suppress over-shoot in the V_{CPD}, RF oscillation becomes stable at a high power level of more than 1 MW. The gyrotron was improved by installing an RF absorber in the beam tunnel, and the output power and pulse duration are enhanced up to 1.1 MW for 3.2 s because of suppression of the parasitic oscillation, while the output power was limited at 1 MW for 2 s without the RF absorber. After re-alignment of transmission lines, moderate transmission efficiencies from gyrotrons to antennas are obtained around 70–80 %. The capability of the RF components equipped in the transmission line has been also demonstrated at a power density of ~1000 MW/m^2.

In conclusion, the improvements of power supply operation, gyrotrons and transmission line alignment have enabled us to obtain the design values of the ECRF system, ~2.8 MW for 2.8 s, and central electron temperatures of ~13 keV are observed by a high power ECRF electron heating experiment in an R-S plasma with ITB.

Acknowledgement

The authors would like to express their thanks to the members of RF Facilities Division who have contributed to the operation of the ECRF system.

References

[1] K. Sakamoto *et al.*, J. Plasma Fusion Res. **71**, 1029 (1995).
[2] K. Sakamoto *et al.*, Review Sci. Instrum. **70**, 208 (1999).
[3] Y. Ikeda *et al.*, Fusion Eng. Des. **53**, 351 (2001).
[4] A. Kasugai *et al.*, Fusion Eng. Des. **53**, 399 (2001).
[5] K. Kajiwara *et al.*, J. Plasma Fusion Res. SERIES, Vol. **3**, 372 (2000).
[6] S. Moriyama, *et al.*, Proc. 14th Top. Conf. Appl. of RF Power to Plasmas, May, 2001, Oxnard.
[7] H. Shoyama *et al.*, J. J. Appl. Phys. **40**, L906 (2001).